ELSEVIER

Journal of Alloys and Compounds 374 (2004) 298–302

Journal of ALLOYS AND COMPOUNDS

www.elsevier.com/locate/jallcom

Enhanced imaging properties of a Gd^{III} complex with unusually large relaxivity

Nicolas Fatin-Rouge [a], Eva Tóth [a], Réto Meuli [b], Jean-Claude G. Bünzli [a,*]

[a] *Institute of Molecular and Biological Chemistry, Swiss Federal Institute of Technology Lausanne, CH-1015 Lausanne, Switzerland*
[b] *Centre Hospitalier Universitaire Vaudois, Radiodiagnostic, CH-1011 Lausanne, Switzerland*

Abstract

MRI contrast properties of self-aggregated nanoparticles made from Gd^{III} and 1,2,4,5-tetrakis(pyrazol-1-yl-methyl-3-carboxylate)benzene (L) are investigated. Viscosity of GdL_2 suspensions and size-characteristics of GdL_2 nanoparticles allow an estimate of their large rotational correlation time. Moreover, two to three H_2O molecules are bound, on average, to Gd^{III} ions, as deduced from ^{17}O NMR titration of the Dy^{III} analogue. The large relaxivity of the particles, along with the prominent peak in the range 20–60 MHz, are the consequence of these two properties. Longitudinal (r_1) and transverse (r_2) relaxivities are determined as a function of monomer concentration at 20 °C and 20 MHz. The ratio r_1/r_2 appears to be favorable for MR imaging using T_1-weighted gradient echo sequences. According to preliminary tests conducted under physiological conditions, the GdL_2 nanoparticles have some potential as contrast agent provided their stability can be increased.

Keywords: Gadolinium; Podate; Relaxivity; Magnetic resonance imaging; Hydration number

1. Introduction

Trivalent gadolinium is well-known to locally create a strong contrasting effect in magnetic resonance imaging (MRI) by increasing the longitudinal and transverse proton relaxation rates of the water molecules in close contact with it [1]. This technique is finding an increasing number of applications both in medical diagnostics and analyses [2]. Among the various parameters affecting the relaxivity, the most important are [3]: the number of water molecules coordinated onto the paramagnetic ion and their exchange rate; the electronic relaxation rate of the paramagnetic ion, and the rotational correlation time around the Gd^{3+}–OH_2 bond. The latter parameter influences significantly the relaxivity profile in the Larmor frequency range 10–100 MHz. Theoretically, the relaxivity versus frequency curve should present a peak of relaxivity, whose theoretical value should culminate at approximately 100–200 $mM^{-1}\,s^{-1}$ for large Gd-containing particles [4].

While a first generation of contrast agents has taken advantage of the thermodynamic and kinetic stability of simple chelates such as $[Gd(dota)]^-$ or $[Gd(dtpa)]^{2-}$, a second generation of molecules is presently being designed, with the aim of developing smart properties such as specific sensing [5] or targeting [6], or very high relaxivity [7]. In particular, the latter is needed for angiography for which it is necessary to create a strong contrast within a short time, compatible with the retention time of the contrast agent in the blood. The main efforts to design high relaxivity contrast agents have relied on increasing the rotational correlation time by using either specific association of the paramagnetic probe with proteins [8], or its insertion into large edifices such as dendrimers [9], micelles [10], or aggregates with low critical aggregation concentrations. We have chosen the latter approach and have demonstrated that the Gd^{III} podates with 1,2,4,5-tetrakis(pyrazol-1-yl-methyl-3-carboxylate)benzene (L) self-aggregate in water to yield nanoparticles with well defined sizes (10, 60 and 280 nm, critical aggregation concentrations: cac-1 $= 3.5 \times 10^{-5}$ M and cac-2 $= 10^{-4}$ M) and that suspensions of these particles present a relaxivity which is about ten times larger than that of the first generation contrast agents [11]. In this paper, we determine the average number of water molecules per lanthanide ion, the rotational correlation time τ_R, as well as r_1 and r_2 NMRD profiles of $\{[GdL_2(H_2O)_q]^{5-}\}_n$ suspensions (abbreviated GdL_2) under MRI experimental conditions, in order to get more insight into their properties and to assess their feasibility for in vivo applications.

* Corresponding author.
E-mail address: jean-claude.bunzli@epfl.ch (J.-C.G. Bünzli).

0925-8388/$ – see front matter © 2003 Elsevier B.V. All rights reserved.
doi:10.1016/j.jallcom.2003.11.125

2. Experimental

2.1. Synthesis and materials

The tetradentate podand L and its complexes were synthesized as previously described [11]. Lanthanide salts were prepared from 99.99% oxide (Rhône-Poulenc) and the corresponding analytical grade acid. Concentrations were determined by complexometric titrations using standardized Na_2H_2edta solutions in urotropine buffered medium and xylene orange as indicator.

2.2. ^{17}O NMR measurements on the Dy^{III} podate

Suspensions of the $\{[DyL_2(H_2O)_q]^{5-}\}_n$ aggregated podate (DyL_2) were prepared by mixing a solution of L (0.0251 M, pH ∼7) with a freshly prepared solution of $Dy(NO_3)_3$ (0.1525 M) in stoichiometric ratio. The concentrations of the DyL_2 aqueous suspensions used (1 ml) were in the range 7×10^{-4} to 5.0×10^{-3} M and the pH was adjusted to 7.5. Dy^{III}-induced ^{17}O chemical shifts (δ) of H_2O from $[Dy(H_2O)_8]^{3+}$ were calibrated versus the metal concentration before determining the shifts of DyL_2 versus concentration. Measurements were carried out on a DPX-600 Bruker NMR spectrometer ($B = 14.1$ T, internal reference ^{17}O-enriched CH_3NO_2) at both 50 and 25 °C. The average number of H_2O molecules, q, per Dy^{III} ion was obtained using Eq. (1) [12]:

$$\text{dis} = \frac{q\delta c}{[H_2O]_{\text{solv}}} \tag{1}$$

where δ is the mean chemical shift of bound water ^{17}O nucleus (obtained from the calibration curve) and c the concentration of the complex. Since at the concentrations used $[H_2O]_{\text{solv}}$ is nearly constant, a linear relationship is expected between dis and c with a slope $q\delta$.

2.3. Viscosity measurements

Viscosity measurements of GdL_2 suspensions ($[GdL_2]_{\text{tot}} = 1.1 \times 10^{-4}$ M) were carried out with an Ostwald capillary viscometer calibrated at 20.0 °C with four fluids (water, ethanol, methanol, heptane). Calibration was performed by using Eq. (2) from flow-rate measurements and knowing the viscosity and density of the four reference fluids.

$$\eta/\rho = At - B/t \tag{2}$$

with η being the viscosity (cps), ρ the density (g/l), t the time (s), while A and B are adjustable parameters. Viscosities were measured versus T (280–345 K) in order to estimate the rotation correlation time (τ_R) of the nanoparticles by using the Stokes–Einstein–Debye [13] Eq. (3), giving τ_R for spherical particles as a function of the suspension viscosity:

$$\tau_R\ (\text{s}) = \frac{4\pi r^3 \eta}{3k_B T} \tag{3}$$

with r (m) being the effective hydrodynamic radius of the particle, η (Pa s) the solution viscosity, T (K) the temperature, and k_B (Pa m^3 K^{-1}) the Boltzmann constant.

2.4. Longitudinal (r_1) and transverse (r_2) proton relaxivity from MRI sequences

Contrast measurements by MRI of GdL_2 suspensions at pH 7.4 were carried out on a MRI Symphony Siemens device ($B = 1.5$ T) at 20 °C and 63 MHz proton Larmor frequency. Relaxation times, T_i ($i = 1, 2$) were obtained by measuring the image contrast (from black to white) versus time after an initial excitation pulse and by adjusting the experimental values with exponential functions $I_i = I_{0,i}(1-\exp(-t/T_i))$, with $i = 1, 2$. For T_1 measurements, three time delays were used (350, 1000 and 2000 ms) and relaxivity was readjusted by using the known value for Omniscan®. Only estimates for r_1 could therefore be obtained from such a procedure and were used to confirm the more precise data extracted from NMRD profiles [11]. For T_2 measurements, twelve time delays were used (from 22.5 to 360 ms with 22.5 ms-intervals). Calculated values of r_i (mM^{-1} s^{-1}) were obtained by adjusting $1/T_i$ values versus $[Gd]_{\text{tot}}$ (mM) according to:

$$\left(\frac{1}{T_i}\right)_{\text{meas}} = \left(\frac{1}{T_i}\right)_{\text{water}} + r_i\,[Gd]_{\text{tot}} \tag{4}$$

3. Results and discussion

Following our previous study [11], we have attempted to determine the number of coordinated water molecules per lanthanide ion, q, in the aggregated nanoparticles using a luminescence lifetime method with Ln = Eu^{III} and Tb^{III}. Data were however not precise enough so that we could only estimate $q \approx 3$ for TbL_2. In order to get a more accurate value, we have turned to another method based on the ^{17}O dysprosium-induced NMR shifts (dis). Indeed, these shifts are dominated by the contact contribution (usually >85%) and are almost independent of the nature of the ligand(s) coordinated to Dy^{III}. Therefore, the mean shift per bound water molecule δ may be determined from a calibration curve based on the aquo-ion ($q = 8$) and measurement of dis versus the complex concentration yields the q value. Some caution has to be taken since q may vary with the chelate concentration. In our case, we have found a linear relationship between the dis in $\{DyL_2(H_2O)_q]^{5-}\}_n$ and the concentration of the aggregated nanoparticles in the range 7×10^{-4} to 5.0×10^{-3} M, meaning that q remains constant in this concentration range. The number of bound H_2O molecules amounts to $q = 1.9 \pm 0.3$. This allows us to get some insight into the coordination environment of the Ln^{III} ion. Assuming a coordination number of 8 for Dy^{III}, the presence of two inner-sphere water molecules implies that the ligand probably acts as a tridentate host. Therefore, since Gd^{III} has the tendency of having a larger

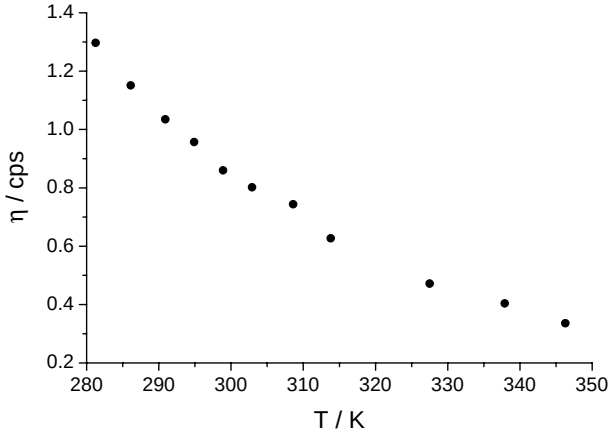

Fig. 1. Viscosity of a GdL_2 suspension versus temperature; $[GdL_2]_{tot} = 1.1 \times 10^{-4}$ M; pH 7.4.

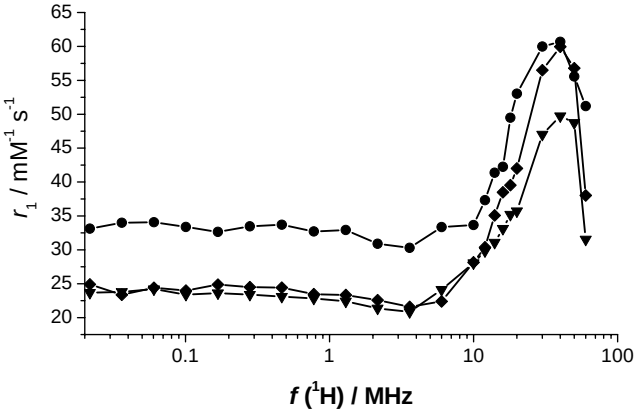

Fig. 2. NMRD profiles of GdL_2 at 5 °C (◆), 25 °C (●), and 75 °C (▼). $[GdL_2]_{tot} = 1.5 \times 10^{-3}$ M; pH 7.2 (pipes). Redrawn from [11].

coordination number than Dy^{III}, a reasonable estimate for the mean number of coordinated water molecules per Gd^{III} ion in the GdL_2 particles lies between 2 and 3.

The nanoparticles have a surface-active effect, inducing a decrease in the solution viscosity as the concentration is increased. The dependence of the solution viscosity upon temperature in the range 281–346 K, at the second critical aggregation concentration $[GdL_2]_{tot} = 1.1 \times 10^{-4}$ M, is presented on Fig. 1. At this concentration, most of the nanoparticles are spherical and have a diameter between 10 and 20 nm, as demonstrated both by light scattering measurements and transmission electron microscopy [11]. Taking this information into account, the rotation correlation time τ_R can be estimated, from the viscosity dependence upon temperature, to lie in the range 100 ns–1 μs (see Eq. (3)). This is apparently a very large value, about two orders of magnitude larger than those reported, on the basis of NMR measurements, for nano-scale edifices such as dendrimers (τ_R = 1–10 ns) or the adduct between a Gd^{III} complex with dotp and human serum albumin HSA (τ_R = 3 ns, radius ~5 nm) [14]. However, it is known that Eq. (3) provides τ_R values one order of magnitude larger than those obtained from ^{17}O or ^{13}C NMR data [15]. The reason is that NMR, as opposed to viscosity, is directly sensitive to the internal motions of the molecules themselves. Therefore, the range of τ_R values extracted from our data for the GdL_2 particles can be considered to be compatible with the one found for the adduct with HSA, the remaining difference being related to the larger size of the GdL_2 particles.

The NMRD-profile of a GdL_2 suspension is reported on Fig. 2 [11]. The high field peak in the range 20–60 MHz is a consequence of the slow rotational correlation time of the self-aggregates; indeed, superparamagnetic properties can be excluded in the present edifices. The decrease of η (and therefore τ_R) versus temperature displayed in Fig. 1 explains, at least partly, why r_1 values are lower at 75 than at 25 °C. Apart of this, the decrease of r_1 observed between 25 and 5 °C, is the signature of a relaxivity limited by a slow water exchange rate [7,14]: the residence time is long compared to the relaxation time. Interest in large particles with contrast agent ability, such as those generated in GdL_2 suspensions, stems from their long retention time in blood, needed for angiographic applications. Another advantage of GdL_2 aggregates lies in the fact that the nanoparticles generate a large and almost constant relaxivity in the frequency range 30–50 MHz, which remains sizable at 63 MHz (30–50 nm^{-1} s^{-1}), which is important for biomedical applications. Many of the known supramolecular systems have a sharper relaxivity peak around 20 MHz followed by an abrupt drop at higher frequencies. Another potential asset of GdL_2 lies in the diameters of the two main kinds of nanoparticles found at concentrations feasible for imaging, 10 and 60 nm. This is well below 100 nm, a limit pertaining to intravenous injections since larger particles are easily retained by the liver. Finally, we have shown that addition of an equimolar quantity of Zn^{II} does not affect the relaxivity [11].

In order to better assess the potentiality of GdL_2 nanoparticles for in vivo MRI analyses, we have determined the longitudinal (T_1) and transverse (T_2) relaxation times of the water protons of GdL_2 suspensions under MRI conditions. The MRI images (Fig. 3) were obtained under clinical experimental conditions by inserting a double-wheeled support fitted with 15 test tubes (1 cm diameter and 10 cm long) into one of the MRI scanners of the University Hospital. We have tested 10 different concentrations of GdL_2, from 10^{-5} M (tube 1) to 10^{-3} M (tube 11) and compared these suspensions to water (tube 12), the Gd^{3+} aquo-ion 10^{-3} M (tube 13) and to two concentrations of the commercial contrast agent Omniscan® (tubes 14, 15). Qualitatively, the brightness of the spots generated by the GdL_2 suspensions increases with concentration to reach a maximum in the range (0.9–2.0) $\times 10^{-4}$ M and then decreases with increasing concentration. The data confirm the laboratory results reported previously [11] in that a 10^{-4} M suspension of GdL_2 has approximately the same effect than a 5×10^{-3} M solution of Omniscan®. More quantitatively, the relaxivity

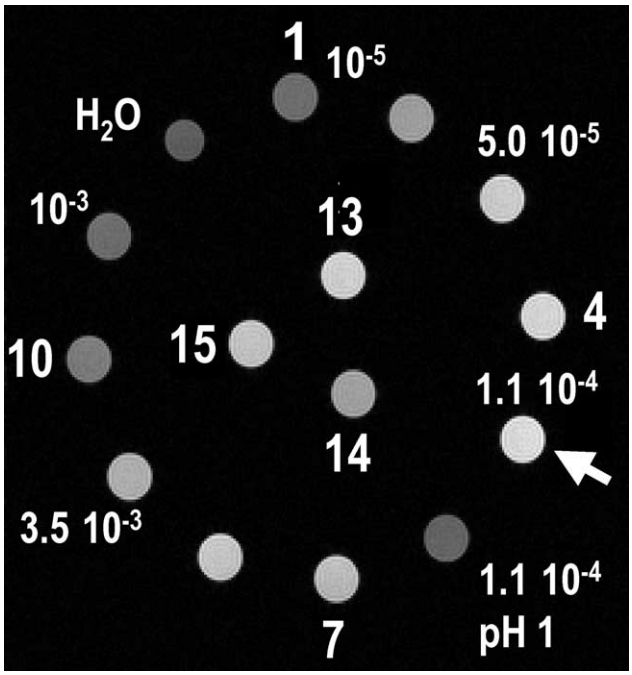

Fig. 3. MRI T_1-images obtained for GdL_2 suspensions at pH 7.4 (unless otherwise indicated) and reference solutions. Tubes 1–11: $[GdL_2]_{tot} = (1; 3; 5; 9; 11; 11\ (pH\ 1); 15; 20; 35; 70; 100) \times 10^{-5}$ M; tube 12: water; tube 13: Gd_{aq}^{3+} 1.1×10^{-4} M, pH 1; tubes 14 and 15: Omniscan® 2.5 and 5×10^{-3} M. Proton Larmor frequency 63 MHz, time delay 2 s.

r_1 can be estimated from its dependence with respect to the concentration (see Fig. 4). In fact, r_1 increases linearly up to cac-2 and reach $40 \pm 2\ mM^{-1}\ s^{-1}$ in the concentration range $(1.1–3.5) \times 10^{-4}$ M, before leveling off and slightly decreasing with concentration. This behavior follows the classical concentration effect exhibited by Gd-based compounds [16]. The dependence of $1/T_2$ upon the concentration of the nanoparticles follow closely the one found for $1/T_1$, except at the highest concentrations (7×10^{-4} to 10^{-3} M) at which $1/T_2$ continues to increase. This explains the lower

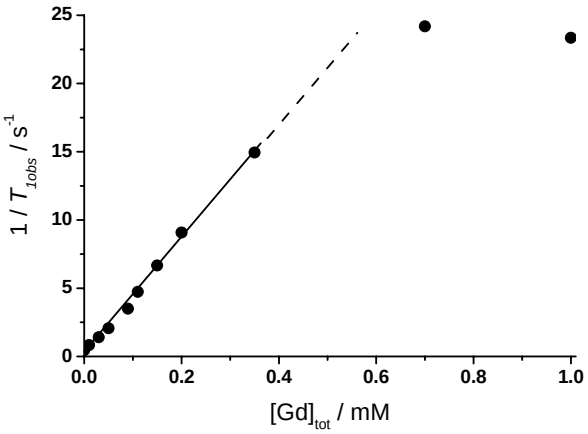

Fig. 4. $1/T_1$ vs. $[Gd]_{tot}$ for aqueous suspensions as measured at 63 MHz, pH 7.4 and $T = 20\,°C$.

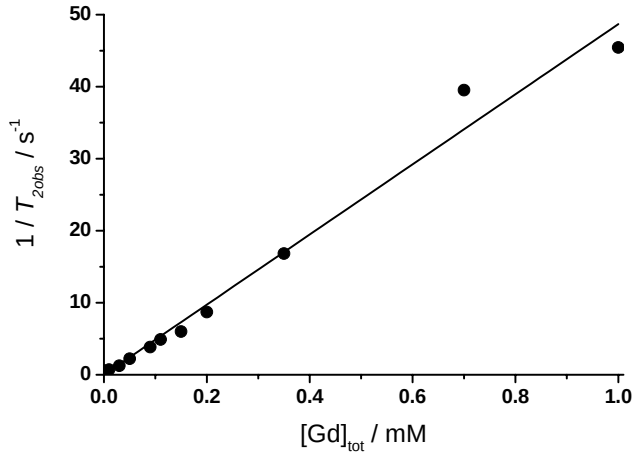

Fig. 5. $1/T_2$ vs. $[Gd]_{tot}$ for aqueous suspensions as measured at 63 MHz, pH 7.4 and $T = 20\,°C$.

contrast observed for the corresponding suspensions (see Figs. 3 and 5). The following mean relaxivity is estimated up to $[GdL_2]_{tot} = 7 \times 10^{-4}$ M: $r_2 = 49 \pm 2\ mM^{-1}\ s^{-1}$, as compared to $3.7\ mM^{-1}\ s^{-1}$ for Omniscan®. The r_1/r_2 ratio appears therefore to be favorable for MR imaging using T_1-weighted gradient echo series.

On the other hand, the 1.1×10^{-4} M suspension, acidified to pH 1, 4 h before measurement, displays a very poor contrasting capability, almost comparable to that of pure water, with r_1 equal to $0.5\ mM^{-1}\ s^{-1}$. By comparison, the uncomplexed aquo-ion $[Gd(H_2O)_n]^{3+}$ at the same concentration and pH displays a relaxivity $r_1 = 21.5\ mM^{-1}\ s^{-1}$. It can be concluded that the pH lowering induces dramatic changes in the Gd^{3+} environment, but that the metal ion is not released into solution. This somewhat surprising behavior will be investigated further.

4. Conclusion

The data presented here clearly point to the large relaxivity exhibited by the GdL_2 nanoparticles in suspension with a high field peak in the range 20–60 MHz being the result of two main factors. First the presence of two to three coordinated water molecules on the metal ion and second the slow rotational correlation time of the rigid 10–20 nm spherical and self-aggregated particles. The transverse electron spin relaxation rate of the GdL_2 nanoparticles, which is around $9 \times 10^9\ s^{-1}$ ($B = 0.34$ T) [11], is a common value which cannot indeed explain the large relaxivity of the GdL_2 suspensions. Concentration studies show that GdL_2 nanoparticles display contrast ability over a broad range, even at quite low concentration (10^{-5} M). Moreover, the properties of the GdL_2 particles, particularly the r_1/r_2 ratio, compare well with those of newly proposed contrast agents with high molecular weight, for instance the [Gd(dota)]-dendrimer [9], for which $r_1 = 36\ mM^{-1}\ s^{-1}$ and $r_2 = 45\ mM^{-1}\ s^{-1}$ at

20 MHz and 23 °C; in addition, they are relatively simpler to synthesize. Their good resistance to exchange with Zn^{II} and the absence of cytotoxicity [16] is also an asset. On the other hand, kinetic tests conducted in presence of large amounts of Arsenazo III or NaCl [17] have revealed a too great lability, related to the relatively low pLn value (pEu = 10 [11] as compared to 15.4 for $[Eu(edta)]^{-}$ [18]) and this aspect must be improved before the GdL_2 nanoparticles can be practically used.

Acknowledgements

We thank Guerbet SA for tests about the cytotoxicity and kinetic stability and of the nanoparticles. This research is supported through grants by the Swiss National Science Foundation and the Swiss Federal Office for Education and Research (COST Action D18, Lanthanide Chemistry for Diagnosis and Therapy).

References

[1] A. Merbach, E. Tóth, The Chemistry of Contrast Agents in Medical Magnetic Resonance Imaging, Wiley, New York, 2001.
[2] R.A. Moats, S.E. Fraser, T.J. Meade, Angew. Chem. Int. Ed. Engl. 36 (2002) 726.
[3] E. Tóth, L. Helm, A.E. Merbach, Top. Curr. Chem. 221 (2002) 61.
[4] E. Tóth, L. Helm, K.E. Kellar, A.E. Merbach, Chem. Eur. J. 5 (1999) 1202.
[5] W.H. Li, G. Parigi, M. Fragai, C. Luchinat, T.J. Meade, Inorg. Chem. 41 (2002) 4018.
[6] G.P. Yan, R.X. Zhuo, Y.H. Yang, L.Y. Li, M.L. Liu, C.H. Ye, J. Biol. Comp. Polym. 17 (2002) 139.
[7] R. Muller, B. Raduchel, S. Laurent, J. Platzek, C. Pierart, P. Mareski, L. Van der Elst, Eur. J. Inorg. Chem. 11 (1999) 1949.
[8] P.L. Anelli, I. Bertini, M. Fragai, L. Lattuada, C. Luchinat, G. Parigi, Eur. J. Inorg. Chem. 4 (2000) 625.
[9] G.M. Nicolle, E. Tóth, H. Schmitt-Willich, B. Raduchel, A.E. Merbach, Chem. Eur. J. 8 (2002) 1040.
[10] G.M. Nicolle, E. Toth, K.P. Eisenwiener, H.R. Mäcke, A.E. Merbach, J. Biol. Inorg. Chem. 7 (2002) 757.
[11] N. Fatin-Rouge, E. Tóth, D. Perret, R.H. Backer, A.E. Merbach, J.-C.G. Bünzli, J. Am. Chem. Soc. 122 (2000) 10810.
[12] M.C. Alpoim, A.M. Urbano, C.F.G.C. Geraldes, J.A. Peters, J. Chem. Soc. Dalton Trans. (1992) 463.
[13] R.J. Stokes, D.E. Fennell, Fundamentals of Interfacial Engineering, Wiley-VCH, New York, 1996.
[14] S. Aime, M. Botta, S. Geninatti Crich, G.B. Giovenzana, R. Pagliarin, M. Piccinini, M. Sisti, E. Terreno, J. Biol. Inorg. Chem. 2 (1997) 470.
[15] E. Tóth, D. Pubanz, S. Vauthey, L. Helm, A.E. Merbach, Chem. Eur. J. 12 (1996) 1607.
[16] R.J. Edelman, M.B. Hesselink, J.R. Zlatkin, Clinical Magnetic Resonance Imaging, vol. 1, second ed., Saunders, New York, 1996.
[17] These tests have been conducted by Guerbet SA, Paris.
[18] Y. Galaktionov, K. Astaklov, Zhur. Neorg. Khim. 8 (1963) 460.